

Open quantum random walks: bi-stability on pure states and ballistically induced diffusion.

Michel Bauer [♣], Denis Bernard [♣] and Antoine Tilloy [♣]

[♣] *Institut de Physique Théorique de Saclay [1], CEA-Saclay, 91191 Gif-sur-Yvette, France.*

[♣] *Laboratoire de Physique Théorique de l'Ecole Normale Supérieure,*

CNRS & Ecole Normale Supérieure de Paris, France

(Dated: July 21, 2022)

Open quantum random walks (OQRWs) deal with quantum random motions on the line for systems with internal and orbital degrees of freedom. The internal system behaves as a quantum random gyroscope coding for the direction of the orbital moves. We reveal the existence of a transition, depending on OQRW moduli, in the internal system behaviours from simple oscillations to random flips between two unstable pure states. This induces a transition in the orbital motions from usual diffusion to ballistically induced diffusion with large mean free path and large effective diffusion constant at large time. We also show that mixed states of the internal system are converted into random pure states during the process. We touch upon possible experimental realisations.

PACS numbers: 03.65.Ta, 03.65.Ud, 05.40.-a

Introduction. Random walks [3] are ubiquitous in our understanding of physical phenomena with plethora of applications in biology or economics. They are instrumental in mathematics and computer science. Quantum generalisations have been considered decades ago [4] and they find numerous applications in quantum computation or quantum cryptography [5]. They have recently been experimentally implemented [6]. Drastically influenced by quantum interferences, quantum random walks behave very differently from their classical analogues, for instance they do not diffuse in the same way.

OQRWs were introduced [7] using concepts from dynamical maps [8] aiming at incorporating decoherence effects. They specify random motions of quantum systems with both internal and orbital degrees of freedom (d.o.f), and these moves depend on interactions with quantum coins. Contrary to quantum random walks, OQRWs implement resettings of the quantum coins at each time step, and this difference has profound consequences.

Studying classes of OQRWs we find a transition in their behaviours separating usual diffusions from ballistically induced diffusions with large mean free path between trajectory flips. Of course diffusion is always due to ballistic behaviours at a small enough scale, what matters is the time separation between flips. In OQRWs, these are not due to disordered collisions but to abrupt tilts of the internal gyroscope induced by the interaction with quantum coins and their measurements. Behaviours in the ballistic regime are consequences of random switches of the internal state between unstable pure states.

Open quantum random walks. To be closer to possible experimental realisations and to quantum trajectory theories [9, 10], we define OQRWs using a picture slightly different but equivalent to [7] in which the system interacts recursively with identical quantum coins, called probes [11]. The probe Hilbert space \mathcal{H}_p is chosen to be two dimensional with a specified basis $\{|\pm\rangle_p\}$. At

each time step, the system interacts quantum mechanically with one sample of identically prepared copies of the probe on which a measurement is performed after the interaction period. The system-probe interaction is such that if the out-going probe is measured in the state $|+\rangle_p$ (resp. $|-\rangle_p$) the system moves by one step to the right (resp. to the left) along the line, and this move is accompanied by a modification of the internal d.o.f's. The system position is slave to the measurement out-puts.

Although experimental realisations of OQRWs do not yet exist we may contemplate possible scenarios in which the orbital states $|n\rangle_o$ refer either to energy levels, numbers of photons or localised positions. One may imagine using ions trapped in harmonic potentials, as in [12, 13], each ion being possibly in two states with different angular momenta, and photons as probes. For an appropriately adjusted frequency and linearly polarised in-going photons, the ion-photon interaction may induce internal flips and energy shifts conditioned on the measurements of out-going photons [14]. One may also imagine using cold atoms with internal d.o.f's and localised on potential lattices, as in [6], and probing them coherently with photons [14]. If one is only interested in the internal system [15], a set-up dealing with recursive couplings of a Qbit to series of probe Qbits, as in [16], may be considered.

To make this description concrete, let $\mathcal{H}_{\text{sys}} := \mathcal{H}_c \otimes \mathcal{H}_o$ be the system Hilbert space, with \mathcal{H}_c and \mathcal{H}_o respectively associated to the internal and orbital d.o.f's. We take \mathcal{H}_c finite dimensional and $\mathcal{H}_o \simeq \mathbb{C}^{\mathbb{Z}}$ with orthonormal basis $\{|n\rangle_o, n \in \mathbb{Z}\}$. Let U be the unitary operator acting on $\mathcal{H}_{\text{sys}} \otimes \mathcal{H}_p$ coding for the system-probe interaction. We demand that its action on states $|\psi\rangle_c \otimes |n\rangle_o \otimes |\phi\rangle_p$ gives the entangled normalised states

$$(B_+|\psi\rangle_c) \otimes |n+1\rangle_o \otimes |+\rangle_p + (B_-|\psi\rangle_c) \otimes |n-1\rangle_o \otimes |-\rangle_p,$$

for any $|\psi\rangle_c \in \mathcal{H}_c$. Unitarity imposes $B_+^\dagger B_+ + B_-^\dagger B_- = \mathbb{I}$.

OQRWs consist in iterating system-probe interactions

and out-going probe measurements. Since the latter are random with probabilities governed by quantum mechanics, this yields stochastic evolutions called quantum trajectories [9, 10]. If the system density matrix is initially localised in the orbital space, say $\rho_0 \otimes |x_0\rangle_o\langle x_0|$, it remains so after each iteration with internal density matrix ρ_n and orbital position x_n . These are randomly updated,

$$\rho_n \otimes |x_n\rangle_o\langle x_n| \rightarrow \frac{B_{\pm}\rho_n B_{\pm}^{\dagger}}{p_n^{\pm}} \otimes |x_n \pm 1\rangle_o\langle x_n \pm 1|, \quad (1)$$

with probability $p_n^{\pm} := \text{tr}_{\mathcal{H}_c}(B_{\pm}\rho_n B_{\pm}^{\dagger})$. The process $n \rightarrow (\rho_n, x_n)$ is Markovian on a probability space whose events are the recursive out-put probe measurements. By construction the mean system density matrix evolves according to the OQRW quantum dynamical map [7], and the mean internal density matrix $\bar{\rho}_n := \mathbb{E}[\rho_n]$ satisfies $\bar{\rho}_{n+1} = B_+\bar{\rho}_n B_+^{\dagger} + B_-\bar{\rho}_n B_-^{\dagger}$. In absence of internal d.o.f's OQRW behaviours parallel those of classical random walks. We take $\mathcal{H}_c \simeq \mathbb{C}^2$ and represent the internal system by an effective spin one-half gyroscope.

Heuristics. Solutions of the unitary constraint may be parametrised as $B_{\pm} = U_{\pm}M_{\pm}$ with U_{\pm} unitary and M_{\pm} hermitian with $M_+^2 + M_-^2 = \mathbb{I}$. These are the OQRW moduli. In the numerical simulations we look for OQRWs generated by $B_+ = \delta^{-1} \begin{pmatrix} u & r \\ s & v \end{pmatrix}$ and $B_- = \delta^{-1} \begin{pmatrix} -v & s \\ r & -u \end{pmatrix}$ with $\delta = \sqrt{u^2 + v^2 + r^2 + s^2}$, and in the scaling limit by $B_{\pm} = \frac{1}{\sqrt{2}}[\mathbb{I} \pm \sqrt{\epsilon}N + \epsilon(iH_{\pm} \pm M - \frac{1}{2}N^{\dagger}N) + o(\epsilon)]$ with ϵ a small parameter and H_{\pm} , M hermitian but not N . We take $H := \frac{1}{2}(H_+ + H_-) = \omega_0 \sigma^2$ and $N = a \sigma^3$ with $\sigma^{1,2,3}$ the usual Pauli matrices.

Numerical simulations reveal the existence of different regimes for OQRWs corresponding to a^2/ω_0 below or above a critical value. For a^2/ω_0 small enough, the position x_n is nearly brownian and the internal density matrix ρ_n oscillates almost regularly, see Fig.2. More interesting behaviours occur for a^2/ω_0 above the critical value, see Fig.1. The position x_n follows a random seesaw trajectory, with tiny fluctuations, whose slopes are determined by the internal state which fluctuates around two unstable fixed points and toggles randomly from one to the other. The abrupt changes in the position moves are due to the random flips of the internal gyroscope. The parameter a^2/ω_0 controls the mean free path between flips. Although ballistic on this time scale, the position is diffusive on larger time scale. Whatever the initial value, the internal density matrix converges rapidly to pure states, so that the fixed points are also pure states. It is quite remarkable that series of indirect probe measurements project mixed states on pure states. The progressive collapses elegantly observed in [17], and proved in [18], is a particular illustration of this phenomena, but in OQRW context the target states keep on evolving randomly.

This peculiar behaviour bears similarities with that of a noisy particle in a double well potential subject to Kramer's transitions from one well to the other. This is

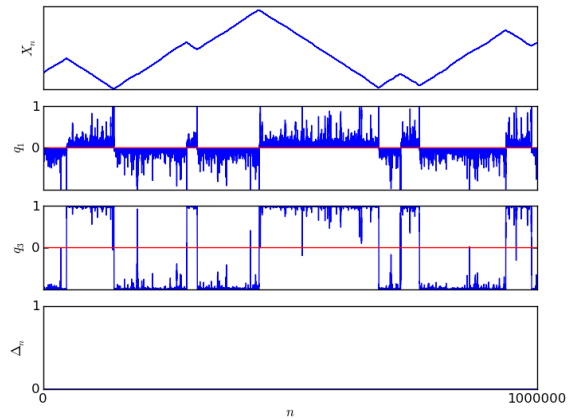


FIG. 1: OQRW generated by B_{\pm} as in the text with $u = 1.1$, $v = 1.00$ and $r = -s = 0.00015$: (a) position X_t , (b)&(c) σ^1 & σ^3 -components of ρ_t , (d) determinant Δ_t .

the picture that we are going to make explicit in the following. The convergence towards pure states can be understood as follows. Let $\Delta_n := \det \rho_n$ be the determinant of the internal density matrix. It vanishes for pure states. A simple computation shows that $\mathbb{E}[\Delta_n^{1/2}] = c^n \Delta_0^{1/2}$ with $c := \det^{\frac{1}{2}}(M_+^2) + \det^{\frac{1}{2}}(M_-^2) < 1$, and $\lim_{n \rightarrow \infty} \mathbb{E}[\Delta_n^{1/2}] = 0$. Actually we can prove that $\lim_{n \rightarrow \infty} \Delta_n^{1/2} = 0$ almost surely using the sub-martingale convergence theorem of probability theory [19]. Indeed, computing the mean of $\Delta_{n+1}^{1/2}$ conditioned on the n -first out-put measurements gives $\mathbb{E}[\Delta_{n+1}^{1/2} | \mathcal{F}_n] = c \Delta_n^{1/2} < \Delta_n^{1/2}$, so that $\Delta_n^{1/2}$ is a sub-martingale, and since it is bounded, it converges almost surely and in \mathbb{L}^1 . The limit is zero and the internal density matrix localises on pure states. As numerically observed, the convergence is very fast.

In a continuous limit, the mean system density matrix reads $\int dx \rho(x, t) \otimes |x\rangle_o\langle x|$ with $p(x, t) := \text{tr}_{\mathcal{H}_c} \rho(x, t)$ the probability density to find the system at position x at time t , and $\bar{\rho}_t := \int dx \rho(x, t)$ the mean internal state. At each time step dt , it is updated using OQRW rules (1),

$$\rho(x, t + dt) = B_- \rho(x + dx, t) B_-^{\dagger} + B_+ \rho(x - dx, t) B_+^{\dagger}.$$

A continuous limit exists if one imposes the scaling relation $\epsilon = dt = dx^2$ [20]. Taylor expansion then gives:

$$\partial_t \rho = \frac{1}{2} \partial_x^2 \rho - (N \partial_x \rho + \partial_x \rho N^{\dagger}) + i[H, \rho] + L_N(\rho), \quad (2)$$

with Lindbladian $L_N(\rho) := N^{\dagger} \rho N - \frac{1}{2}(N N^{\dagger} \rho + \rho N N^{\dagger})$. Eq.(2) mixes pieces from diffusive Fokker-Planck equation and from Lindbladian quantum evolution for $\bar{\rho}_t$ [21]. The term $(N \partial_x \rho + \partial_x \rho N^{\dagger})$ is at the origin of the ballistic behaviour seen in Fig.1 and of the large effective diffusion constant but the hamiltonian term is required for the tilting effect. The probability $p(x, t)$ is not associated to a Markov process and does not satisfy a linear equation but it becomes gaussian at large t .

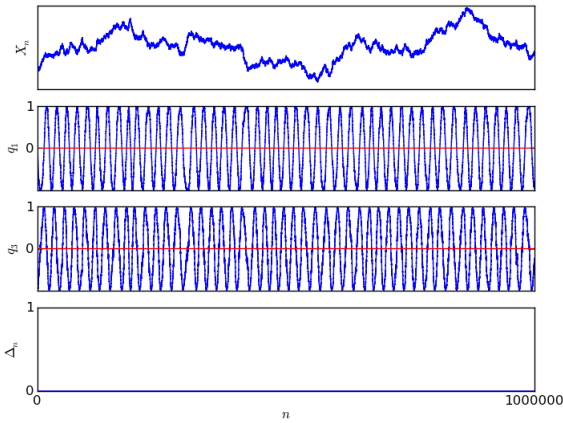


FIG. 2: OQRW generated by B_{\pm} as in the text with $u = 1.005$, $v = 1.00$ and $r = -s = 0.00015$: (a) position X_t , (b)&(c) σ^1 & σ^3 -components of ρ_t , (d) determinant Δ_t .

Scaling limit. Let us now make precise the heuristic description by deriving the stochastic differential equations (SDEs) governing OQRWs in the scaling limit. OQRWs are defined on the probability space whose events are the series (s_1, s_2, \dots) with $s_k = \pm$ depending whether the k -th out-going probe is measured in the state $|\pm\rangle_p$. Functions which depend only on the n first data (s_1, \dots, s_n) define a natural filtration \mathcal{F}_n [19], and $p_n^{\pm} := \mathbb{E}[\mathbb{I}_{\{s_{n+1}=\pm\}} | \mathcal{F}_n] = \text{tr}(B_{\pm} \rho_n B_{\pm}^{\dagger})$ are the probabilities for $s_{n+1} = \pm$ conditioned on the value of the internal state at the n -th step. A quick and neat way to obtain the scaling limit consists in decomposing the process ρ_n as a sum of a martingale M_n plus a predictable process O_n . This is called a Doob decomposition [19]. In the scaling limit the martingale (resp. predictable) contribution converges to the noisy source (resp. the drift) of the SDEs. Eq.(1) may be tautologically written as

$$\rho_{n+1} = \rho_n^{(+)} \mathbb{I}_{\{s_{n+1}=+\}} + \rho_n^{(-)} \mathbb{I}_{\{s_{n+1}=-\}},$$

and $x_{n+1} - x_n = \mathbb{I}_{\{s_{n+1}=+\}} - \mathbb{I}_{\{s_{n+1}=-\}}$, with $\rho_n^{(\pm)} := B_{\pm} \rho_n B_{\pm}^{\dagger} / p_n^{\pm}$. By construction the Doob martingale is $M_n = \sum_{k=1}^n \pi_k$ with $\pi_k := \rho_k - \mathbb{E}[\rho_k | \mathcal{F}_{k-1}]$ given by:

$$2\pi_k = (\rho_k^{(+)} - \rho_k^{(-)}) (\mathbb{I}_{\{s_{k+1}=+\}} - p_k^+ + p_k^- - \mathbb{I}_{\{s_{k+1}=-\}}).$$

The predictable process is defined by complementarity $O_n := \rho_n - M_n$. Taking the scaling limit $\epsilon \rightarrow 0$, $t = n\epsilon$ fixed, is a matter of Taylor expanding $dM_t := M_{n+1} - M_n$, $d\rho_t := \rho_{n+1} - \rho_n$ and $dX_t := \sqrt{\epsilon}(x_{n+1} - x_n)$. Identifying ϵ with dt , we get $dM_t = D_N(\rho_t) dB_t$, and

$$d\rho_t = (i[H, \rho_t] + L_N(\rho_t)) dt + D_N(\rho_t) dB_t, \quad (3)$$

$$dX_t = U_N(\rho_t) dt + dB_t, \quad (4)$$

with B_t a normalised Brownian motion, $D_N(\rho) := N\rho + \rho N^{\dagger} - \rho U_N(\rho)$ and $U_N(\rho_t) := \text{tr}(N\rho + \rho N^{\dagger})$. Not surprisingly, eq.(3) is of Belavkin's type [22, 23]. The drift

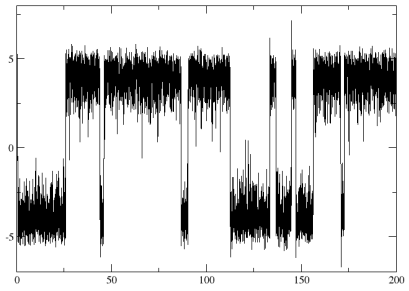


FIG. 3: A y_t -trajectory for $a^2 > \omega_0$.

in eq.(4) is governed by the internal state and this is responsible for the behaviours observed in Figs.1&2.

Bi-stability and ballistic diffusion. We take $H = \omega_0 \sigma^2$ and $N = a \sigma^3$. Eqs.(3,4) are then compatible with reality of the internal density matrix. We parametrise it as $\rho_t = \frac{1}{2}(\mathbb{I} + q_1 \sigma^1 + q_3 \sigma^3)$ with $q_1^2 + q_3^2 \leq 1$. Eqs.(3,4) then reads:

$$\begin{aligned} dq_3 &= 2\omega_0 q_1 dt + 2a(1 - q_3^2) dB_t \\ dq_1 &= -2(\omega_0 q_3 + a^2 q_1) dt - 2a q_1 q_3 dB_t \end{aligned}$$

To check convergence to pure states, let $\Delta_t := \det \rho_t$. We have $d\Delta_t = -4\Delta_t[a^2(1 - q_3^2)dt + aq_3 dB_t]$ with non positive drift so that Δ_t is a sub-martingale [19]. It converges quickly to 0, so we may describe ρ_t as a pure state, $q_1 = \sin \theta$, $q_3 = \cos \theta$. The angle θ satisfies

$$d\theta_t = -2(\omega_0 + a^2 \sin \theta_t \cos \theta_t) dt - 2a \sin \theta_t dB_t \quad (5)$$

The behaviour of θ_t is quantitatively different depending whether $a^2 \gtrless \omega_0$, and this corresponds to the two regimes we mentioned. For $a^2 < \omega_0$, θ_t rotates randomly but regularly enough around the unit circle, so that the internal state ρ_t oscillates almost regularly. For $a^2 > \omega_0$, θ_t is trapped during random periods in the vicinity of $\theta_-^* \simeq 0^-$ or $\theta_+^* \simeq \pi^-$. The points θ_{\pm}^* are the minima of the effective potential obtained from eq.(5) once correctly normalised. Although it fluctuates, θ_t turns predominantly clockwise (for $\omega_0 > 0$) around the unit circle, never crossing back 0 or π anticlockwise.

To make this description quantitative, let $y_t := -\log |\tan \theta_t / 2|$. It satisfies a normalised SDE with constant noise source, $dy_t = 2a dB_t - V'(y_t) dt$ with potential

$$V(y) = -2(\pm \omega_0 \sinh y + 2a^2 \log \cosh y).$$

The above sign is that of $\tan \theta_t / 2$, i.e. $+/-$ for θ_t on the upper/lower half unit circle. What happens in these two sectors is symmetrical, so we concentrate on the upper sector. The potential shape is that of a cubic like function but it is exponentially large for large $|y|$, i.e. $V(y) \simeq -\omega_0 \text{sign}(y) e^{|y|}$. It possesses a minimum and a maximum for $a^2 > \omega_0$, and none if $a^2 < \omega_0$. The minimum is at $y_+^* \simeq -2a^2/\omega_0$ for large a , i.e. $\tan \theta_+^* \simeq e^{-y_+^*}$ so that θ_+^* is close to π^- , with $V_{\min} \simeq -4a^2 \log a^2/\omega_0$

and $V_{\max} \simeq 0$. When θ_t enters the upper sector, it does it from π . For y_t this corresponds to $-\infty$, so that y_t experiences an exponentially steep down ramp that it can never climb back, and this means that θ_t never escapes the upper sector from π but only from 0. Going down on the ramp, y_t reaches the potential minimum and spends time fluctuating around there, and this means that θ_t fluctuates around θ_+^* . At a random time τ_{flip} , large fluctuations allow y_t to cross the energy barrier in a Kramer's like process. Once this has happened, y_t is again on a steep ramp that it steps down to $+\infty$, and this translates to θ_t moving toward 0^+ and crossing it irreversibly towards the lower sector. The process then starts on the lower half circle and repeats itself. See Fig.3. We estimate the mean flip time as $\mathbb{E}[\tau_{\text{flip}}] \simeq e^{\Delta V/4a^2} \simeq a^2$ by Kramer's rule, and a more precise study allows us determine the probability distribution of τ_{flip}/a^2 .

The internal state drives the system position via eq.(4) which reads $dX_t = 2a \cos \theta_t dt + dB_t$. The slopes of the seesaw profiles of X_t are $2a \cos \theta_{\pm}^* \simeq \mp 2a$. Fluctuations are negligible for large a but the noise is instrumental for tilting from one slope to the other via Kramer's transitions. The mean system density matrix heuristically introduced above is rigorously defined by

$$\int dx \rho(x, t) \otimes |x\rangle_o \langle x| := \mathbb{E}[\rho_t \otimes |X_t\rangle_o \langle X_t|]. \quad (6)$$

Routine applications of stochastic Itô calculus [19] show that the SDEs (3,4) imply eq.(2) for $\rho(x, t)$. Eq.(2) is of Lindblad form on $\mathcal{H}_c \otimes \mathbb{L}^2(\mathbb{R})$. It may be used to check that X_t/\sqrt{t} becomes gaussian at large time, in a way compatible with the central limit theorem of [24, 25], and $\mathbb{E}[X_t^2] = D_{\text{eff}} t$ with effective diffusion constant $D_{\text{eff}} = 1 + 4a^4/\omega_0^2$. The factor 1 comes from the bare diffusion constant [20] while the second term, which dominates for large a , is induced by the ballistic seesaws.

Conclusion. The transition from usual diffusion to ballistically induced diffusion is an echo of the internal gyroscope behaviours. In the ballistic regime the internal state switches randomly between two pure states in a way similar to Kramer's transition. Since the system position is slave to the out-put measurements, our results about convergence from a mixed state to pure states and about random flips between them apply to the coupled probe plus internal spin system without considering orbital d.o.f's. More details will be given elsewhere [26]. In the ballistic regime the effective diffusion constant is much larger than the bare one, and one may wonder about other scenarios of ballistically induced diffusion providing large effective diffusion constants. Finally, one may muse about possible applications of the rapid and irreversible internal state flips to switch devices [27]. As such these switches are random but one may imagine changing on demand the height of the energy barrier.

Acknowledgements: This work was in part supported by ANR contract ANR-2010-BLANC-0414. D.B. thanks

J.M. Raimond for discussions, especially on possible experimental scenarios.

-
- [1] CEA/DSM/IPhT, Unité de recherche associée au CNRS
 - [2] Emails: michel.bauer@cea.fr, denis.bernard@ens.fr, antoine.tilloy@ens.fr.
 - [3] W. Feller, *An Introduction to Probability Theory and its Applications*, Wiley, 1968.
 - [4] J. Kempe (2003), *Contemp. Phys.* 44 (2003) 307; S. Venegas-Andraca, arXiv:1201.4680, and refs. therein.
 - [5] M.A. Nielsen, I.L. Chuang, *Quantum computation and quantum information*, Cambridge Univ. Press 2005; R. Blatt, C.F. Roos, *Nature Phys.* 8 (2009) 174.
 - [6] M. Karski et al, *Science* 325 (2009) 174.
 - [7] S. Attal, F. Petruccione, C. Sabot, I. Sinayskiy, *J. Stat. Phys.* 147, 832852 (2012).
 - [8] See e.g. S. Attal, A. Joyce and C.A. Pillet, eds. *Open quantum systems, vol. I, II and III*, Lectures notes in mathematics, vol.1880-1882, Springer, 2006.
 - [9] H.J. Charnichael, *An open system approach to quantum optics*, Lect. Notes Phys. vol.18 (1993), Springer-Berlin.
 - [10] J. Dalibard, Y. Castin and K. Molner, *Phys. Rev. Lett.* 68 (1992) 580; and 1992-preprint [arXiv:0805.4002].
 - [11] In mathematical terms, this defines a dilation of the QORW quantum map, which is reproduced back when tracing out the probe space. On contrary, quantum trajectories emerge when performing probe measurements and keeping track of their out-puts.
 - [12] C. Monroe et al, *Phys. Rev. Lett.* 75 (1995) 4714.
 - [13] J.I. Cirac and P. Zoller, *Phys. Rev. Lett.* 74 (1995) 4091.
 - [14] Obviously, the tremendous experimental problem is to act on trapped ions with a few photons and not with a pulse containing a large number of them.
 - [15] The system position behaves classically if it initially starts localised and if one always measures the probe observable with eigenbasis $|\pm\rangle_p$, as done here. In such case, a quantum implementation of the orbital d.o.f's is not really needed. However, this is clearly a restriction and one could decide either to initially start with a more general state or to measure other observables.
 - [16] H. Häffner, C. Roos, R. Blatt, *Phys. Rep.* 469 (2008) 155.
 - [17] C. Guerlin et al, *Nature* 448 (2007) 889.
 - [18] M. Bauer, D. Bernard, *Phys. Rev.* A84, 044103 (2011).
 - [19] E.g. J. Jacod and Ph. Protter, *L'essentiel en théorie des probabilités*, Cassini, Paris (2003).
 - [20] Here we make a choice of length and time normalisations, and this fixes the bare diffusion constant $D_0 = 1$.
 - [21] G. Lindblad, *Commun. Math. Phys.* 48 (1976) 119-130.
 - [22] A. Barchielli, *Phys. Rev. A* 34 (1986) 1642-1648.
 - [23] V. P. Belavkin, *J. Math. Phys.* 31 (1990) 2930-2934; *Commun. Math. Phys.* 146 (1992) 611-635.
 - [24] S. Attal, N. Guillotin-Plantard, C. Sabot, arXiv:1206.1472.
 - [25] N. Konno, H.J. Yoo, arXiv:1209.1419.
 - [26] M. Bauer, D. Bernard, A. Tilloy, in preparation.
 - [27] These flips are rapid because once on the top of the energy barrier the internal state moves along exponentially steep ramps, and they are irreversible because it never climbs them back.